Impact of nonlinearity and wave dispersion parameters on the soliton pulses of the (2+1)-dimensional Kundu-Mukherjee-Naskar equation

S. M. Rayhanul Islam[a], D. Kumar[b], E. Fendzi-Donfack[c,d], and M. Inc[e,f]

[a]*Department of Mathematics, Pabna University of Science and Technology, Pabna, Bangladesh.*
e-mail: rayhanulmath@yahoo.com
[b]*Department of Mathematics, Bangabandhu Sheikh Mujibur Rahman Science and Technology University, Gopalganj 8100, Bangladesh.*
e-mail: dks.bsmrstu@gmail.com
[c]*Nonlinear Physics and Complex Systems Group, Department of Physics, The Higher Teacher's Training College, University of Yaoundé I, P.O. Box 47, Yaoundé, Cameroon.*
[d]*Pure Physics Laboratory, Group of Nonlinear Physics and Complex Systems, Department of Physics, Faculty of Sciences, University of Douala, P.O. Box 24157, Douala, Cameroon.*
e-mail: fendziemmanuel@yahoo.fr
[e]*Biruni University, Department of Computer Engineering, Istanbul, Turkey.*
[f]*Department of Medical Research, China Medical University, Taichung, Taiwan.*
e-mail: minc@firat.edu.tr

Received 12 February 2022; accepted 19 May 2022

In this study, we explain the impact of nonlinearity and wave dispersion parameters on the soliton pulses of the (2+1)-dimensional Kundu-Mukherjee-Naskar equation. In this regard, some new optical solitons are received via the unified method to the aforesaid equation to explain such impact on the soliton pulses. The presented optical solitons are expressed by the dark, bright, periodic, bell, kink, and singular soliton solutions. Considering both effects help stabilize the soliton pulses during their propagation by generating new dynamics depending upon the nonlinearity and the wave dispersion parameters of the studied equation. All the characteristics of the soliton pulses are exhibited graphically. It is found from the graphical outputs that the soliton profiles are decreasing and increasing with the increase of nonlinearity and dispersion parameters, respectively. The outcomes reveal that the soliton pulses are balanced due to the influences of nonlinearity and wave dispersion parameters of the aforementioned equation. It is mentioned that the impact of wave dispersion and nonlinearity parameters on the soliton pulses has not been discussed before. Therefore, the applied method permits the explanation of the various wave dynamics by analyzing the attained soliton solutions in nonlinear optical fibers systems, which can be used for further studies.

Keywords: KMN equation; unified method; soliton pulse; wave dispersion; nonlinearly.

DOI: https://doi.org/10.31349/RevMexFis.68.061301

1. Introduction

1.1. *Background and literature review*

It is well known that the nonlinear Schrödinger equation (NLSE) explains the underlying mechanism broadly in numerous fields, such as quantum mechanics [1], plasma physics [2], nonlinear optics [3], optical fibers [4, 5], fluid dynamics [6], and hydrodynamics [7]. The related research of the NLSE has mainly focused on their results in fiber optic communication systems. Kundu-Mukherjee-Naskar (KMN) equation is one of the equations that explain the hidden phenomena in the aforementioned fields. More specifically, the KMN equation can be used in fiber amplifiers, optical fiber, data transmission, and so on. Recently, many scholars have studied the different forms of the NLSE about Kerr and non-Kerr law nonlinearities to study optical soliton by using powerful techniques, such as the modified simple equation method [8], the sine-Gordon expansion method [9], the extended simple equation method [10], the modified analytical method [11], the modified Kudryashov method [12] and so on.

In 2013, Kundu and Mukherjee [13] studied the integrable higher-dimensional NLSE and described its features, solutions, and applications. One year later, the KMN equation was first introduced by Kundu *et al.* [14], which is a new extension of the NLSE (See in section 1.3). The KMN model is the most important model for describing the rough ocean waves and noticeably (2+1)-dimensional characteristics. This model can also be used to propagate light waves through coherently excited resonant waveguides, especially in the case of bending light [15]. Moreover, this model can be useful for the learning of isolated pulses in the (2+1)-dimensional equation [16]. Recently, many scholars have been addressed the exact solutions of the KMN model by using different techniques, such as the first integral method [17], the method of undetermined coefficients and Lie symmetry [18], the trial equation technique [19], the modified simple equation approach [20], the new extended algebraic

method [21], the ansatz approach and the sine Gordon expansion method [22], the F-expansion and functional variable methods [23], the new extended direct algebraic method [24], and the exp-function method [25]. Very recently, Kumar *et al*. [26] discussed the effects of fractional parameters and wave obliqueness of the KMN model by analyzing the soliton pulses, obtained via the generalized Kudryashov and the new auxiliary equation methods. It is noteworthy to mention here that dark, bright, singular, singular period, rough wave, bell, anti-bell type soliton solutions are reported in the previous literature. However, the impacts of wave dispersion and nonlinearity parameters on soliton pulses of the KMN model have not been investigated, as well as the unified method applications' to the KMN equation.

1.2. Objective of the study

The main goal of this research is to apply the unified method for exploring some new optical solitons, such as dark, bright, periodic, and singular soliton solutions to an integrable KMN equation, which can be of great significance in the field of fiber optics and optical communications. It is noted to mention here that optical solitons are solitary light waves that hold their form over an expansive interval, which produce crystal clear phone calls cross-country and internationally. Furthermore, we will also explain the impacts of wave dispersion and nonlinearity on the attained soliton pulses of the KMN model.

1.3. Mathematical model

In this study, we consider the following (2+1) dimensional KMN equation [14–26] as

$$iu_t + \sigma u_{xy} + i\kappa\left(uu_x^* - u^* u_x\right) = 0, \quad i = \sqrt{-1}. \tag{1}$$

In Eq. (1), the spatial variables are represented by x and y, the time variable stands on t, the dependent variable $u(x, y, t)$ is the nonlinear wave envelope and $u^*(x, y, t)$ is represented by the complex conjugate of $u(x, y, t)$. The second term in Eq. (1) represents the evolution of the wave followed by the wave dispersion term that is given by the coefficient of σ.

The constant κ ensures the existence of the different case of nonlinearity media which does not fall into the conventional Kerr law nonlinearity or any known non-Kerr law media [16]. The nonlinear term in this equation accounts for "current-like" nonlinearity that stems from chirality [20]. The utmost significant feature of the (2+1)-dimensional KMN model is that it has been given as a new extension of the nonlinear Schrödinger (NLS) equation with the inclusion of different forms of nonlinearity with regard to Kerr and non-Kerr law nonlinearities to study soliton pulses.

1.4. Arrangement of the study

The rest of the paper is organized as follows: the overview of the unified method is presented in Sec. 2. Mathematical analysis is presented in Sec. 3. Graphical analysis of the obtained solutions and the impacts of wave dispersion and nonlinearity on soliton pulses are discussed in Sec. 4. Finally, we give a general conclusion in Sec. 5.

2. Overview of the unified method

The unified method [27, 28] is the amalgamation of all hyperbolic tangent function methods, such as the tanh-function scheme, the extended tanh-function technique, the modified extended tanh-function method, and the complex tanh function scheme. In Ref. [28], Gozukizil *et al*., explored the analytic solution to the Rabinovich wave equation and compared between the family of tanh function method and unified method. Besides, they compared the tanh method [29–31], the extended tanh method [32], the modified extended tanh method [33], and the complex tanh-function method [34] with results generated with the unified method. Later, Akcagil and Aydemir [34] applied the unified method to the Lonngren wave equation. They proved that the unified method gives many more general solutions in an elegant way than the family of the tanh-function methods [29–31] and the family of (G'/G)-expansion method, and the $(G'/G, 1/G)$-expansion method. Besides the unified method, many other methods have been applied for obtaining analytic solutions for NLEEs, such as the (G'/G^2)-expansion method [35], the Hirota bilinear method [36, 37], the sine-Gordon equation method [38], the extended sinh-Gordon equation expansion method [39], the enhanced (G'^2/G)-expansion method [40–42], the $\exp(-\phi(\xi)$-expansion method [43], the modified simple equation [44], the improved F-expansion method [44], the new ϕ^6-model expansion method [45], the generalized bilinear method [46], the extended Fan sub-equation technique [47], and many more.

The main overviews of the unified method are as follows. Consequently, we consider the general form of the nonlinear partial differential equation as

$$L\left(u, u_t, u_x, u_y, u_{tt}, u_{xx}, u_{yy}, u_{xt}, u_{xy}, u_{yt}, ...\right) = 0. \tag{2}$$

Using wave transformation

$$u(x, y, t) = u(\Omega), \quad \Omega = x + y - vt, \tag{3}$$

where v is the traveling wave. Inserting Eq. (3) into Eq. (2) yields the following ODE:

$$K(u, u^{'}, u^{''}, ...) = 0. \tag{4}$$

Let us consider that Eq. (4) has the following solutions:

$$u(\Omega) = A_0 + \sum_{j=1}^{T}\left(A_j X^j + B_j X^{-j}\right), \tag{5}$$

where T is the homogeneous balance parameter which can be determined by balancing between highest order linear and

nonlinear terms of Eq. (4), and $X = X(\Omega)$ satisfies the Riccati differential equation as follow:

$$X^{'} = X^{2}(\Omega) + \gamma, \tag{6}$$

where $X^{'} = dX/d\Omega$, A_j, B_j $(j = 1, 2, 3, ..., T)$ and γ are constants. Eq. (6) has the following solutions:
Cluster 01: If $\gamma < 0$, then the hyperbolic function solutions are

$$X(\Omega) = \frac{\sqrt{-(M^2+P^2)\gamma} - M\sqrt{-\gamma}\cosh\left(2\sqrt{-}\gamma(\Omega+\eta)\right)}{M\sinh\left(2\sqrt{-}\gamma(\Omega+\eta)\right)+P}, \tag{7}$$

$$X(\Omega) = \frac{-\sqrt{-(M^2+P^2)\gamma} - M\sqrt{-\gamma}\cosh\left(2\sqrt{-}\gamma(\Omega+\eta)\right)}{M\sinh\left(2\sqrt{-}\gamma(\Omega+\eta)\right)+P}, \tag{8}$$

$$X(\Omega) = \sqrt{-\gamma} - \frac{2M\sqrt{-\gamma}}{M+\cosh\left(2\sqrt{-}\gamma(\Omega+\eta)\right)-\sinh\left(2\sqrt{-}\gamma(\Omega+\eta)\right)}, \tag{9}$$

$$X(\Omega) = -\sqrt{-\gamma} + \frac{2M\sqrt{-\gamma}}{M+\cosh\left(2\sqrt{-}\gamma(\Omega+\eta)\right)+\sinh\left(2\sqrt{-}\gamma(\Omega+\eta)\right)}. \tag{10}$$

Cluster 02: If $\gamma > 0$, then the trigonometric function solutions are

$$X(\Omega) = \frac{\sqrt{(M^2-P^2)\gamma} - M\sqrt{\gamma}\cos\left(2\sqrt{\gamma}(\Omega+\eta)\right)}{M\sin\left(2\sqrt{\gamma}(\Omega+\eta)\right)+P}, \tag{11}$$

$$X(\Omega) = \frac{-\sqrt{(M^2-P^2)\gamma} - M\sqrt{\gamma}\cos\left(2\sqrt{\gamma}(\Omega+\eta)\right)}{M\sin\left(2\sqrt{\gamma}(\Omega+\eta)\right)+P}, \tag{12}$$

$$X(\Omega) = i\sqrt{\gamma} - \frac{2iM\sqrt{\gamma}}{M+\cos\left(2\sqrt{\gamma}(\Omega+\eta)\right)-i\sin\left(2\sqrt{\gamma}(\Omega+\eta)\right)}, \tag{13}$$

$$X(\Omega) = -i\sqrt{\gamma} + \frac{2iM\sqrt{\gamma}}{M+\cos\left(2\sqrt{\gamma}(\Omega+\eta)\right)+i\sin\left(2\sqrt{\gamma}(\Omega+\eta)\right)}. \tag{14}$$

Cluster 03: If $\gamma = 0$, then the rational function solution is

$$X(\Omega) = -\frac{1}{\Omega+\eta}, \tag{15}$$

where $M, P \in \mathbb{R}$ and η is an arbitrary constant.
We put Eqs. (5) and (6) in Eq. (4) and associating all the coefficient of $X^i = -N \leq i \leq N$ to zero yield a set of algebraic equations for A_j, B_j and γ. Putting A_j, B_j, Ω and γ into Eq. (5) and using the general solutions of Eq. (6), it can be obtained the solutions of Eq. (2) directly based on the value of γ.

3. Mathematical analysis

Let us consider the complex wave transformation as follows

$$u(x, y, t) = U(\Omega)\, e^{i\psi(x,y,t)}. \tag{16}$$

In Eq. (16), the amplitude and phase element of the soliton are $U(\Omega)$ and $\psi(x, y, t)$ respectively, where $\Omega = ax - by - vt$ and $\psi = -px - qy + mt + m_0$. Here, p and q represent the frequencies of the soliton in the x and y directions respectively, whereas m and m_0 signifies the wave number and phase of the soliton respectively. In addition, the parameters a and b in Eq. (16) represent the inverse width of the soliton with x and y directions, respectively and v represents the speed of the soliton. Plugging the above transformation into Eq. (1) and equating real and imaginary parts, we attained the following equations:

$$\sigma abU^{''} - (m + \sigma pq)\, U - 2\kappa pU^3 = 0, \tag{17}$$

and

$$v = -\sigma(pb + qa). \tag{18}$$

Applying the balance statement on Eq. (17), yields $T = 1$. So, the solution of Eq. (17) can be expressed in the following form:

$$U(\Omega) = A_0 + A_1 X(\Omega) + B_1 X(\Omega)^{-1}. \tag{19}$$

Among them, A_0, A_1, and B_1 are constant to be determined later and the function $X(\Omega)$ satisfies the Eq. (6). Inserting Eq. (19) along with Eq. (6) into Eq. (17) and collecting all terms with the same power of $X(\Omega)$ together, equating each coefficient to zero yields a set of algebraic equations in terms of A_0, A_1, B_1 and m. The following solution sets are obtained:

$$\text{Set one:} \quad m6 = -2\sigma ab - \sigma pq, \quad A_0 = 0, \quad A_1 = \pm\sqrt{\frac{\sigma ab}{\kappa p}}, \quad B_1 = 0. \tag{20}$$

$$\text{Set two:} \quad m = 4\sigma ab - \sigma pq, \quad A_0 = 0, \quad A_1 = \pm\sqrt{\frac{\sigma ab}{\kappa p}}, \quad B_1 = \pm\sqrt{\frac{\sigma ab}{\kappa p}}. \tag{21}$$

$$\text{Set three:} \quad m = -2\sigma ab - \sigma pq, \quad A_0 = 0, \quad A_1 = 0, \quad B_1 = \pm\sqrt{\frac{\sigma ab}{\kappa p}}. \tag{22}$$

Inserting Eqs. (20)–(22) into Eq. (19) along with the Eqs. (7)–(10), one can attain the following hyperbolic function solutions:

Group one:

$$u_{1,2}(x,y,t) = \pm e^{i\psi(x,y,t)}\sqrt{\frac{\sigma ab}{\kappa p}}\left(\frac{\sqrt{-(M^2+P^2)\gamma} - M\sqrt{-\gamma}\cosh\left(2\sqrt{-}\gamma(\Omega+\eta)\right)}{M\sinh\left(2\sqrt{-}\gamma(\Omega+\eta)\right)+P}\right),$$

$$u_{3,4}(x,y,t) = \pm e^{i\psi(x,y,t)}\sqrt{\frac{\sigma ab}{\kappa p}}\left(\frac{-\sqrt{-(M^2+P^2)\gamma} - M\sqrt{-\gamma}\cosh\left(2\sqrt{-}\gamma(\Omega+\eta)\right)}{M\sinh\left(2\sqrt{-}\gamma(\Omega+\eta)\right)+P}\right),$$

$$u_{5,6}(x,y,t) = \pm e^{i\psi(x,y,t)}\sqrt{\frac{\sigma ab}{\kappa p}}\left(\sqrt{-\gamma} - \frac{2M\sqrt{-\gamma}}{M+\cosh\left(2\sqrt{-}\gamma(\Omega+\eta)\right)-\sinh\left(2\sqrt{-}\gamma(\Omega+\eta)\right)}\right),$$

$$u_{7,8}(x,y,t) = \pm e^{i\psi(x,y,t)}\sqrt{\frac{\sigma ab}{\kappa p}}\left(-\sqrt{-\gamma} + \frac{2M\sqrt{-\gamma}}{M+\cosh\left(2\sqrt{-}\gamma(\Omega+\eta)\right)+\sinh\left(2\sqrt{-}\gamma(\Omega+\eta)\right)}\right),$$

where $\Omega = ax + by + \sigma(pb + qa)t$ and $\psi = -px - qy + (2\gamma\sigma ab - \sigma pq)t + m_0$.

Group two:

$$u_{9,10}(x,y,t) = \pm e^{i\psi(x,y,t)}\sqrt{\frac{\sigma ab}{\kappa p}}\left(\frac{\sqrt{-(M^2+P^2)\gamma} - M\sqrt{-\gamma}\cosh\left(2\sqrt{-}\gamma(\Omega+\eta)\right)}{M\sinh\left(2\sqrt{-}\gamma(\Omega+\eta)\right)+P} + (R_0)^{-1}\right),$$

$$u_{11,12}(x,y,t) = \pm e^{i\psi(x,y,t)}\sqrt{\frac{\sigma ab}{\kappa p}}\left(\frac{-\sqrt{-(M^2+P^2)\gamma} - M\sqrt{-\gamma}\cosh\left(2\sqrt{-}\gamma(\Omega+\eta)\right)}{M\sinh\left(2\sqrt{-}\gamma(\Omega+\eta)\right)+P} + (R_1)^{-1}\right),$$

$$u_{13,14}(x,y,t) = \pm e^{i\psi(x,y,t)}\sqrt{\frac{\sigma ab}{\kappa p}}\left(\sqrt{-\gamma} - \frac{2M\sqrt{-\gamma}}{M+\cosh\left(2\sqrt{-}\gamma(\Omega+\eta)\right)-\sinh\left(2\sqrt{-}\gamma(\Omega+\eta)\right)} + (R_2)^{-1}\right),$$

$$u_{15,16}(x,y,t) = \pm e^{i\psi(x,y,t)}\sqrt{\frac{\sigma ab}{\kappa p}}\left(-\sqrt{-\gamma} + \frac{2M\sqrt{-\gamma}}{M+\cosh\left(2\sqrt{-}\gamma(\Omega+\eta)\right)+\sinh\left(2\sqrt{-}\gamma(\Omega+\eta)\right)} + (R_3)^{-1}\right),$$

where

$$R_0 = \frac{\sqrt{-\left(M^2+P^2\right)\gamma} - M\sqrt{-\gamma}\cosh\left(2\sqrt{-}\gamma\left(\Omega+\eta\right)\right)}{M\sinh\left(2\sqrt{-}\gamma\left(\Omega+\eta\right)\right)+P},$$

$$R_1 = \frac{-\sqrt{-\left(M^2+P^2\right)\gamma} - M\sqrt{-\gamma}\cosh\left(2\sqrt{-}\gamma\left(\Omega+\eta\right)\right)}{M\sinh\left(2\sqrt{-}\gamma\left(\Omega+\eta\right)\right)+P},$$

$$R_2 = \sqrt{-\gamma} - \frac{2M\sqrt{-\gamma}}{M+\cosh\left(2\sqrt{-}\gamma\left(\Omega+\eta\right)\right)-\sinh\left(2\sqrt{-}\gamma\left(\Omega+\eta\right)\right)},$$

$$R_3 = -\sqrt{-\gamma} + \frac{2M\sqrt{-\gamma}}{M+\cosh\left(2\sqrt{-}\gamma\left(\Omega+\eta\right)\right)+\sinh\left(2\sqrt{-}\gamma\left(\Omega+\eta\right)\right)},$$

$$\Omega = ax+by+\sigma(pb+qa)t \quad and \quad \psi = -px-qy+(2\gamma\sigma ab-\sigma pq)t+m_0.$$

Group three:

$$u_{17,18}\left(x,y,t\right) = \pm e^{i\psi(x,y,t)}\sqrt{\frac{\sigma ab}{\kappa p}}\left(\frac{\sqrt{-\left(M^2+P^2\right)\gamma} - M\sqrt{-\gamma}\cosh\left(2\sqrt{-}\gamma\left(\Omega+\eta\right)\right)}{M\sinh\left(2\sqrt{-}\gamma\left(\Omega+\eta\right)\right)+P}\right)^{-1},$$

$$u_{19,20}\left(x,y,t\right) = \pm e^{i\psi(x,y,t)}\sqrt{\frac{\sigma ab}{\kappa p}}\left(\frac{-\sqrt{-\left(M^2+P^2\right)\gamma} - M\sqrt{-\gamma}\cosh\left(2\sqrt{-}\gamma\left(\Omega+\eta\right)\right)}{M\sinh\left(2\sqrt{-}\gamma\left(\Omega+\eta\right)\right)+P}\right)^{-1},$$

$$u_{21,22}\left(x,y,t\right) = \pm e^{i\psi(x,y,t)}\sqrt{\frac{\sigma ab}{\kappa p}}\left(\sqrt{-\gamma} - \frac{2M\sqrt{-\gamma}}{M+\cosh\left(2\sqrt{-}\gamma\left(\Omega+\eta\right)\right)-\sinh\left(2\sqrt{-}\gamma\left(\Omega+\eta\right)\right)}\right)^{-1},$$

$$u_{23,24}\left(x,y,t\right) = \pm e^{i\psi(x,y,t)}\sqrt{\frac{\sigma ab}{\kappa p}}\left(-\sqrt{-\gamma} + \frac{2M\sqrt{-\gamma}}{M+\cosh\left(2\sqrt{-}\gamma\left(\Omega+\eta\right)\right)+\sinh\left(2\sqrt{-}\gamma\left(\Omega+\eta\right)\right)}\right)^{-1},$$

where $\Omega = ax+by+\sigma(pb+qa)t$ and $\psi = -px-qy+(2\gamma\sigma ab-\sigma pq)t+m_0$.

Inserting Eqs. (20)–(22) into Eq. (19) along with the Eqs. (11)–(14), one can attain the following trigonometric function solutions:

Group four:

$$u_{25,26}\left(x,y,t\right) = \pm e^{i\psi(x,y,t)}\sqrt{\frac{\sigma ab}{\kappa p}}\left(\frac{-\sqrt{\left(M^2-P^2\right)\gamma} - M\sqrt{\gamma}\cos\left(2\sqrt{\gamma}\left(\Omega+\eta\right)\right)}{M\sin\left(2\sqrt{\gamma}\left(\Omega+\eta\right)\right)+P}\right),$$

$$u_{27,28}\left(x,y,t\right) = \pm e^{i\psi(x,y,t)}\sqrt{\frac{\sigma ab}{\kappa p}}\left(\frac{-\sqrt{\left(M^2-P^2\right)\gamma} - M\sqrt{\gamma}\cos\left(2\sqrt{\gamma}\left(\Omega+\eta\right)\right)}{M\sin\left(2\sqrt{\gamma}\left(\Omega+\eta\right)\right)+P}\right),$$

$$u_{29,30}\left(x,y,t\right) = \pm e^{i\psi(x,y,t)}\sqrt{\frac{\sigma ab}{\kappa p}}\left(i\sqrt{\gamma} - \frac{2iM\sqrt{\gamma}}{M+\cos\left(2\sqrt{\gamma}\left(\Omega+\eta\right)\right)-i\sin\left(2\sqrt{\gamma}\left(\Omega+\eta\right)\right)}\right),$$

$$u_{31,32}\left(x,y,t\right) = \pm e^{i\psi(x,y,t)}\sqrt{\frac{\sigma ab}{\kappa p}}\left(-i\sqrt{\gamma} + \frac{2iM\sqrt{\gamma}}{M+\cos\left(2\sqrt{\gamma}\left(\Omega+\eta\right)\right)+i\sin\left(2\sqrt{\gamma}\left(\Omega+\eta\right)\right)}\right),$$

where $\Omega = ax+by+\sigma(pb+qa)t$ and $\psi = -px-qy+(2\gamma\sigma ab-\sigma pq)t+m_0$.

Group five:

$$u_{33,34}(x,y,t) = \pm e^{i\psi(x,y,t)}\sqrt{\frac{\sigma ab}{\kappa p}}\left(\frac{\sqrt{(M^2-P^2)\gamma} - M\sqrt{\gamma}\cos\left(2\sqrt{\gamma}\,(\Omega+\eta)\right)}{M\sin\left(2\sqrt{\gamma}\,(\Omega+\eta)\right)+P} + (R_4)^{-1}\right),$$

$$u_{35,36}(x,y,t) = \pm e^{i\psi(x,y,t)}\sqrt{\frac{\sigma ab}{\kappa p}}\left(\frac{-\sqrt{(M^2-P^2)\gamma} - M\sqrt{\gamma}\cos\left(2\sqrt{\gamma}\,(\Omega+\eta)\right)}{M\sin\left(2\sqrt{\gamma}\,(\Omega+\eta)\right)+P} + (R_5)^{-1}\right),$$

$$u_{37,38}(x,y,t) = \pm e^{i\psi(x,y,t)}\sqrt{\frac{\sigma ab}{\kappa p}}\left(i\sqrt{\gamma} - \frac{2iM\sqrt{\gamma}}{M+\cos\left(2\sqrt{\gamma}\,(\Omega+\eta)\right)-i\sin\left(2\sqrt{\gamma}\,(\Omega+\eta)\right)} + (R_6)^{-1}\right),$$

$$u_{39,40}(x,y,t) = \pm e^{i\psi(x,y,t)}\sqrt{\frac{\sigma ab}{\kappa p}}\left(-i\sqrt{\gamma} + \frac{2iM\sqrt{\gamma}}{M+\cos\left(2\sqrt{\gamma}\,(\Omega+\eta)\right)+i\sin\left(2\sqrt{\gamma}\,(\Omega+\eta)\right)} + (R_7)^{-1}\right),$$

where

$$R_4 = \frac{\sqrt{(M^2-P^2)\gamma} - M\sqrt{\gamma}\cos\left(2\sqrt{\gamma}\,(\Omega+\eta)\right)}{M\sin\left(2\sqrt{\gamma}\,(\Omega+\eta)\right)+P},$$

$$R_5 = \frac{-\sqrt{(M^2-P^2)\gamma} - M\sqrt{\gamma}\cos\left(2\sqrt{\gamma}\,(\Omega+\eta)\right)}{M\sin\left(2\sqrt{\gamma}\,(\Omega+\eta)\right)+P},$$

$$R_6 = i\sqrt{\gamma} - \frac{2iM\sqrt{\gamma}}{M+\cos\left(2\sqrt{\gamma}\,(\Omega+\eta)\right)-i\sin\left(2\sqrt{\gamma}\,(\Omega+\eta)\right)},$$

$$R_7 = -i\sqrt{\gamma} + \frac{2iM\sqrt{\gamma}}{M+\cos\left(2\sqrt{\gamma}\,(\Omega+\eta)\right)+i\sin\left(2\sqrt{\gamma}\,(\Omega+\eta)\right)},$$

$$\Omega = ax+by+\sigma(pb+qa)t \quad \text{and} \quad \psi = -px-qy+(-4\gamma\sigma ab-\sigma pq)t+m_0.$$

Group six:

$$u_{41,42}(x,y,t) = \pm e^{i\psi(x,y,t)}\sqrt{\frac{\sigma ab}{\kappa p}}\left(\frac{\sqrt{(M^2-P^2)\gamma} - M\sqrt{\gamma}\cos\left(2\sqrt{\gamma}\,(\Omega+\eta)\right)}{M\sin\left(2\sqrt{\gamma}\,(\Omega+\eta)\right)+P}\right)^{-1},$$

$$u_{43,44}(x,y,t) = \pm e^{i\psi(x,y,t)}\sqrt{\frac{\sigma ab}{\kappa p}}\left(\frac{-\sqrt{(M^2-P^2)\gamma} - M\sqrt{\gamma}\cos\left(2\sqrt{\gamma}\,(\Omega+\eta)\right)}{M\sin\left(2\sqrt{\gamma}\,(\Omega+\eta)\right)+P}\right)^{-1},$$

$$u_{45,46}(x,y,t) = \pm e^{i\psi(x,y,t)}\sqrt{\frac{\sigma ab}{\kappa p}}\left(i\sqrt{\gamma} - \frac{2iM\sqrt{\gamma}}{M+\cos\left(2\sqrt{\gamma}\,(\Omega+\eta)\right)-i\sin\left(2\sqrt{\gamma}\,(\Omega+\eta)\right)}\right)^{-1},$$

$$u_{47,48}(x,y,t) = \pm e^{i\psi(x,y,t)}\sqrt{\frac{\sigma ab}{\kappa p}}\left(-i\sqrt{\gamma} + \frac{2iM\sqrt{\gamma}}{M+\cos\left(2\sqrt{\gamma}\,(\Omega+\eta)\right)+i\sin\left(2\sqrt{\gamma}\,(\Omega+\eta)\right)}\right)^{-1},$$

where $\Omega = ax+by+\sigma(pb+qa)t$ and $\psi = -px-qy+(2\gamma\sigma ab-\sigma pq)t+m_0$.

Inserting Eqs. (20)–(22) into Eq. (19) along with the Eq. (15), one can attain the rational function solutions.

Group seven:

$$u_{49,50}(x,y,t) = \pm e^{i\psi(x,y,t)}\sqrt{\frac{\sigma ab}{\kappa p}}\left(\frac{1}{\Omega+\eta}\right),$$

where $\Omega = ax+by+\sigma(pb+qa)t$ and $\psi = -px-qy-\sigma pqt+m_0$.

4. Graphical illustrations of the attained solutions

In this section, we will discuss the physical behaviors of the solutions obtained from the KMN equation via some graphical illustrations. The impacts of wave dispersion (σ) and nonlinearity (κ) parameters on some attained optical solitons are also presented and explained graphically.

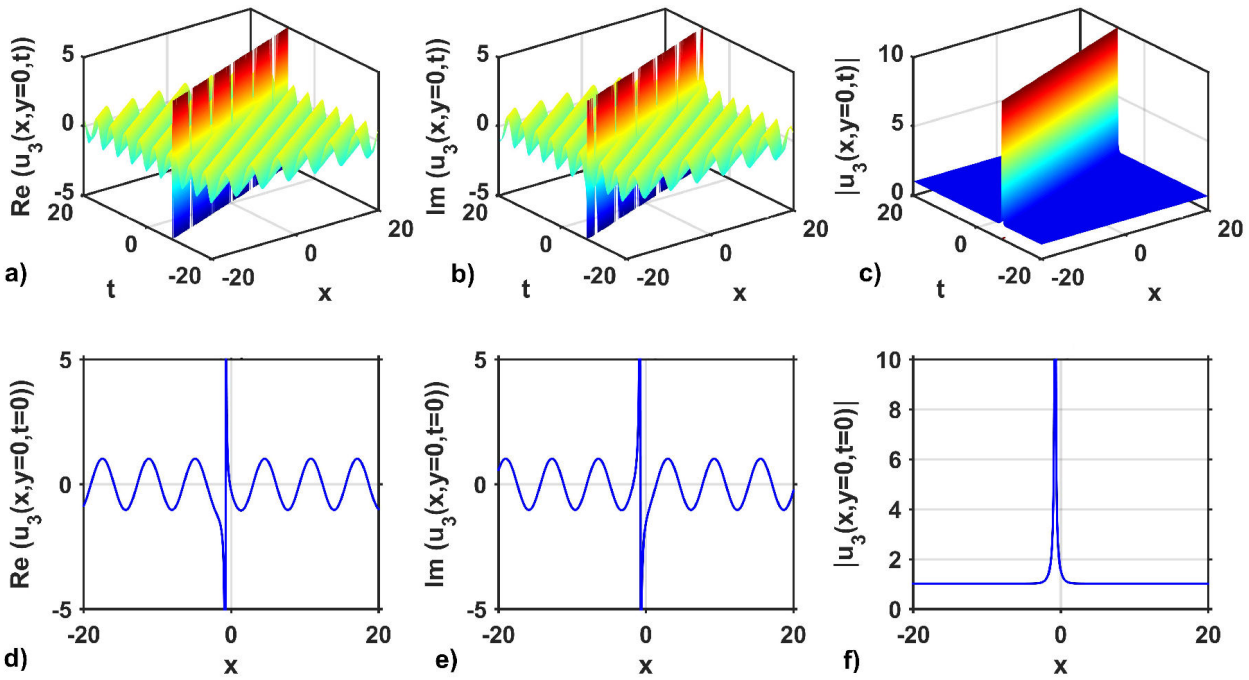

FIGURE 1. 3D structures of the solution $u_3(x, y = 0, t)$: a) real part, b) imaginary part, c) modulus, and d)-f): 2D line plots of a)-c) at $t = 0$, respectively, for selecting the free parameters values as $a = 1.01$, $b = 1$, $\sigma = 1$, $\kappa = 1$, $p = 1$, $q = -3.5$, $M = 1.5$, $P = 1.3$, $\eta = 0.4$, $m_0 = 1.4$ and $\gamma = -1.04$.

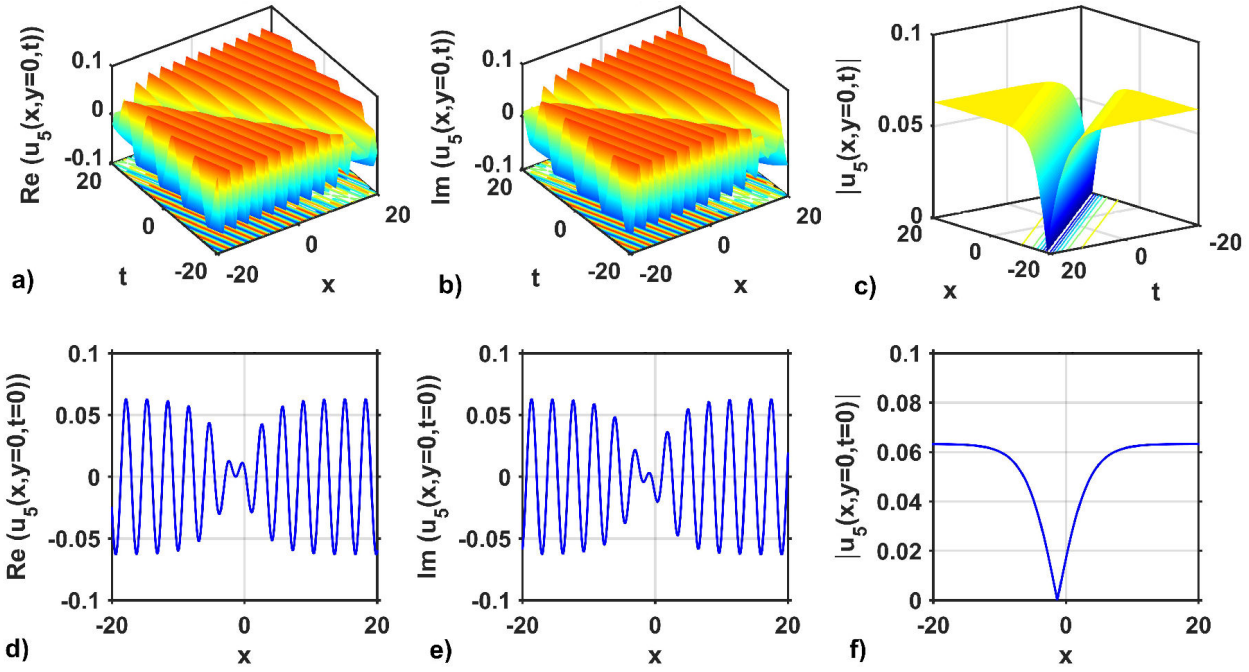

FIGURE 2. 3D structures of the solution $u_5(x, y = 0, t)$: a) real part, b) imaginary part, c) modulus, and d)-f): 2D line plots of a)-c) at $t = 0$, respectively, for selecting the free parameters values as $a = 1.5$, $b = 2$, $\sigma = 0.2$, $\kappa = 1$, $p = 2$, $q = 1.7$, $M = 1.5$, $P = 1.3$, $\eta = 0.5$, $m_0 = 2$ and $\gamma = -0.02$.

4.1. Graphical analysis of the diverse wave solutions

Taking into account the special value of the free parameters, the 3D and 2D wave structures of the solutions obtained from the KMN equation are considered to show the behavior of the solution. In addition, the 3D wave profile is exposed to show the temporal and spatial changes of the obtained optical soliton solution. The 3D wave profile for the real and imaginary parts and modulus of the optical solution $u_1(x, y = 0, t)$ are depicted in Figs. 1a)-c) respectively. The optical solution

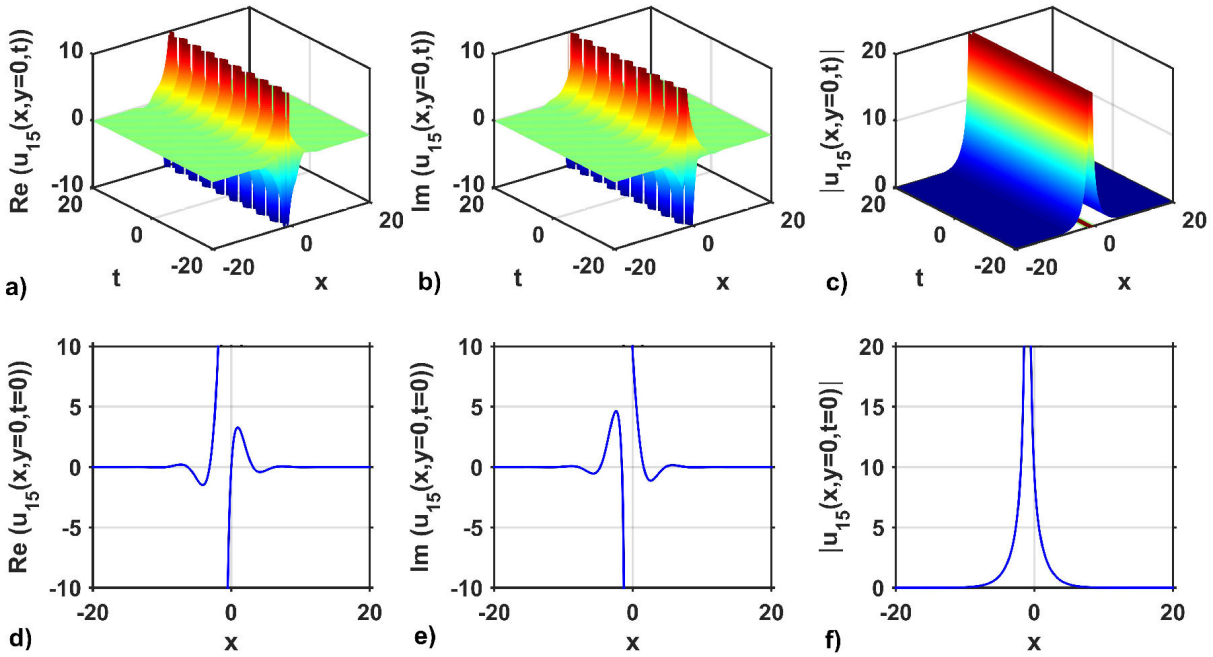

FIGURE 3. 3D structures of the solution $u_15(x, y = 0, t)$: a) real part, b) imaginary part, c) modulus, and d)-f): 2D line plots of a)-c) at $t = 0$, respectively, for selecting the free parameters values as $a = 1$, $b = 1$, $\sigma = 1$, $\kappa = 0.01$, $p = 1$, $q = 1.5$, $M = 1$, $\eta = 1$, $m_0 = 0$ and $\gamma = -0.1$.

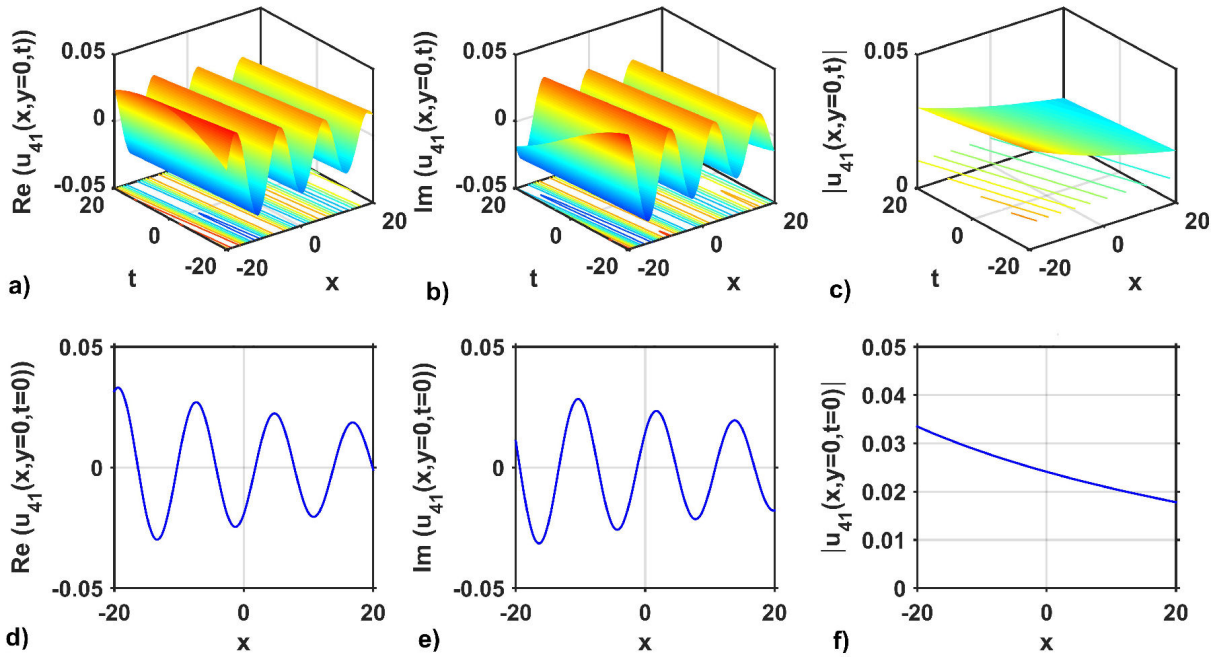

FIGURE 4. 3D structures of the solution $u_41(x, y = 0, t)$: a) real part, b) imaginary part, c) modulus, and d)-f): 2D line plots of a)-c) at $t = 0$, respectively, for selecting the free parameters values as $a = 0.01$, $b = 0.02$, $\sigma = 0.59$, $\kappa = 0.12$, $p = 0.52$, $q = 0.5$, $M = 2.5$, $P = 0.1$, $\eta = 0.9$, $m_0 = 2.5$ and $\gamma = 0.56$.

$u_1(x, y = 0, t)$ represents the periodic wave solution for the real and imaginary parts, as portrayed in Fig. 1a) and b). On the other hand, the modulus of the above solution represents the singular soliton, which is depicted in Fig. 1c). The above mentioned can be confirmed from their 2D cross-sectional views at $t = 0$, as shown in Figs. 1d)-f). The 3D and 2D wave profiles of the optical solution $u_5(x, y = 0, t)$ represent the real and imaginary parts and modulus of the optical solution $u_5(x, y = 0, t)$, as shown in Figs. 2a)-f). The 3D structure of the real and imaginary parts of the optical solution $u_5(x, y = 0, t)$ signifies the periodic wave structure, which is shown in Fig. 2a) and b), however, Fig. 2d) and e)

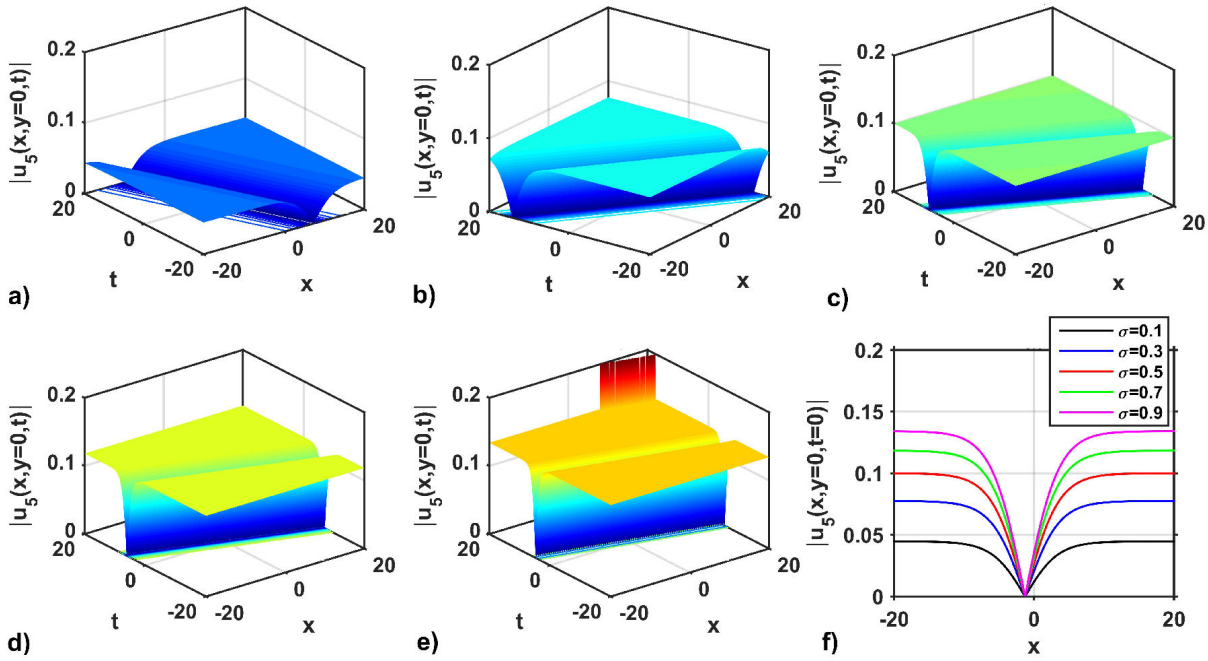

FIGURE 5. Impacts on wave dispersion on the solution $|u_1(x, y = 0, t)|$: a)-e) for $\sigma = 0.1, 0.3, 0.5, 0.7$, and 0.9, respectively, with $a = 2.5$, $b = 0.2$, $\kappa = 0.01$, $p = 2.5$, $q = -2.5$, $M = 0.02$, $P = 0.021$, $\eta = 1$, $m_0 = 1$, $\gamma = -0.25$, and f) the variation of the soliton profiles at $t = 1$ of a)-e) along with x-axis.

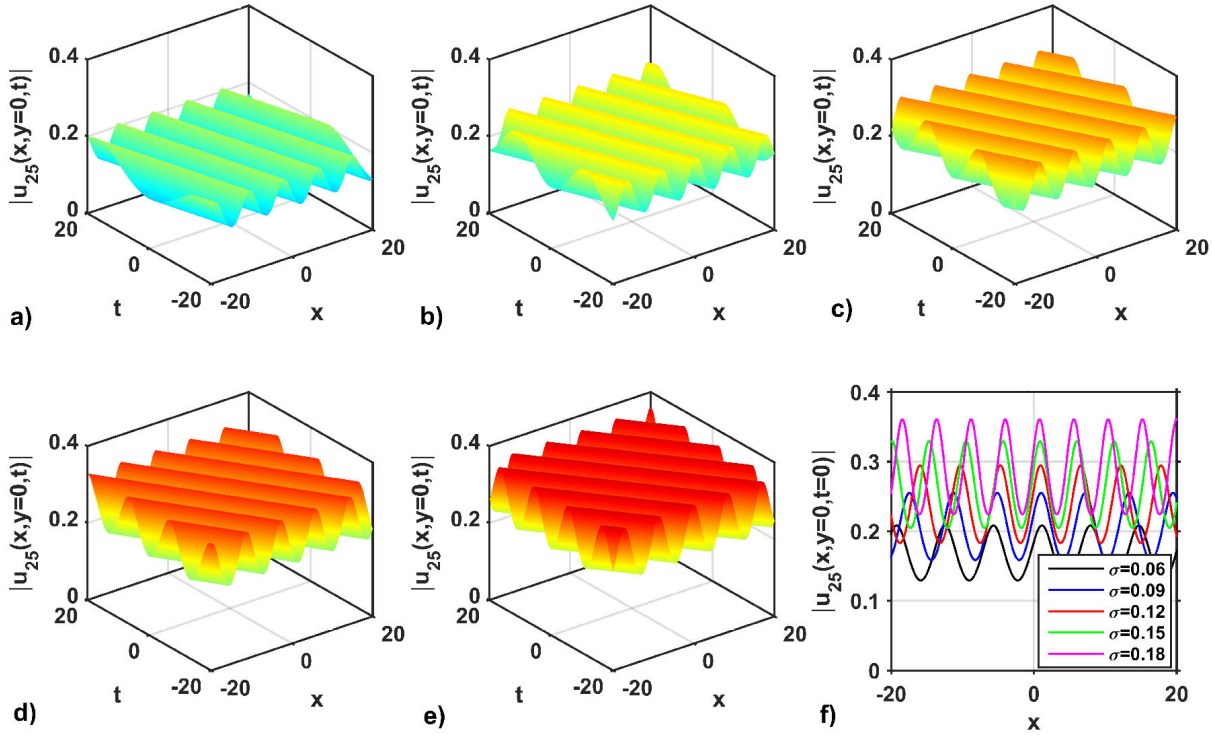

FIGURE 6. Impacts on wave dispersion on the solution $|u_{25}(x, y = 0, t)|$: a)-e) for $\sigma = 0.06, 0.09, 0.12, 0.15$, and 0.18, respectively, with $a = 1.2$, $b = 1$, $\kappa = 1$, $p = 1$, $q = 1$, $M = 0.07$, $P = 0.03$, $\eta = 1.5$, $m_0 = 4.6$, $\gamma = 1.5$, and f) the variation of the soliton profiles at $t = 1$ of a)-e) along with x-axis.

display the 2D line plots of the real and imaginary parts of the mentioned solution at $t = 0$ respectively. The modulus of the optical solution $u_5(x, y = 0, t)$ also demonstrate the anti-bell soliton solution, which is depicted in Fig. 2(c). As shown in Fig. 2f), the 2D graph at $t = 0$ confirms this type of anti-bell soliton solution. Figures 3a)-f) display the 3D and 2D wave

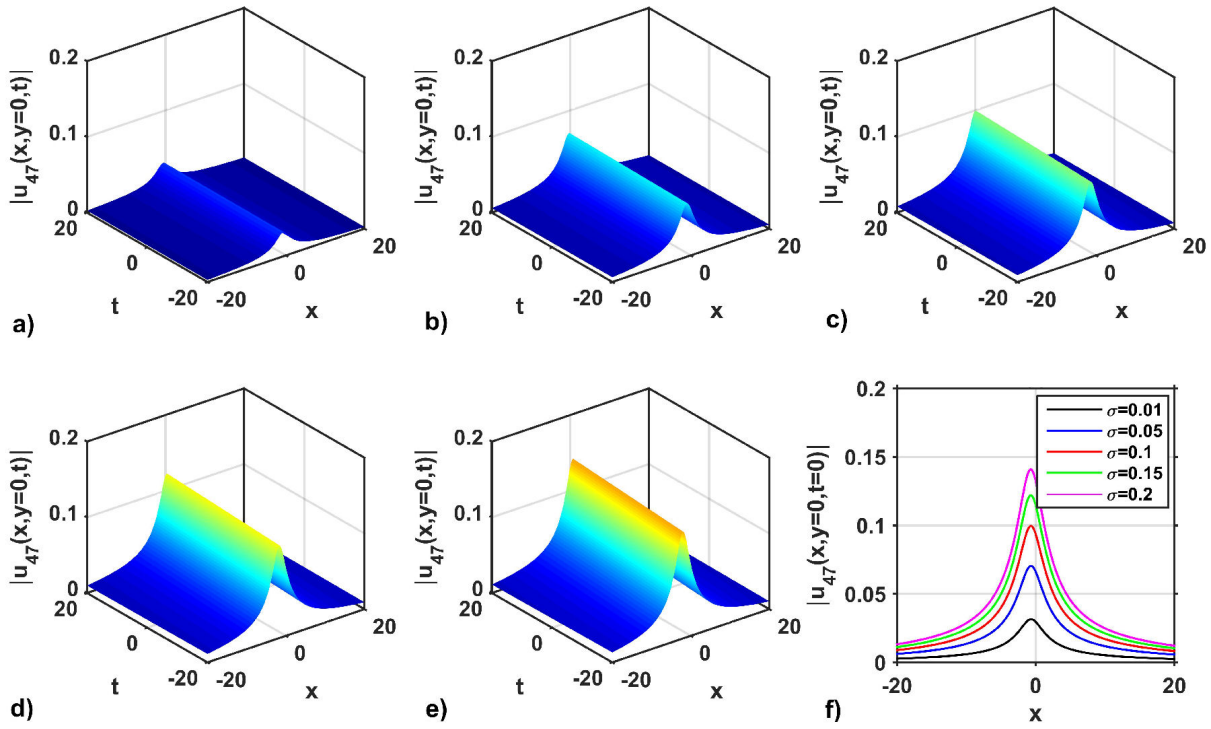

FIGURE 7. Impacts on wave dispersion on the solution $|u_{47}(x, y = 0, t)|$: (a)-(e) for $\sigma = 0.01, 0.05, 0.10, 0.15$, and 0.2, respectively, with $a = 0.15$, $b = 0.1$, $\kappa = 1$, $p = 1$, $q = -1$, $M = 1.1$, $P = 0.1$, $\eta = 0.1$, $m_0 = 1.5$, $\gamma = 0.03$, and (f) the variation of the soliton profiles at $t = 1$ of (a)-(e) along with x-axis.

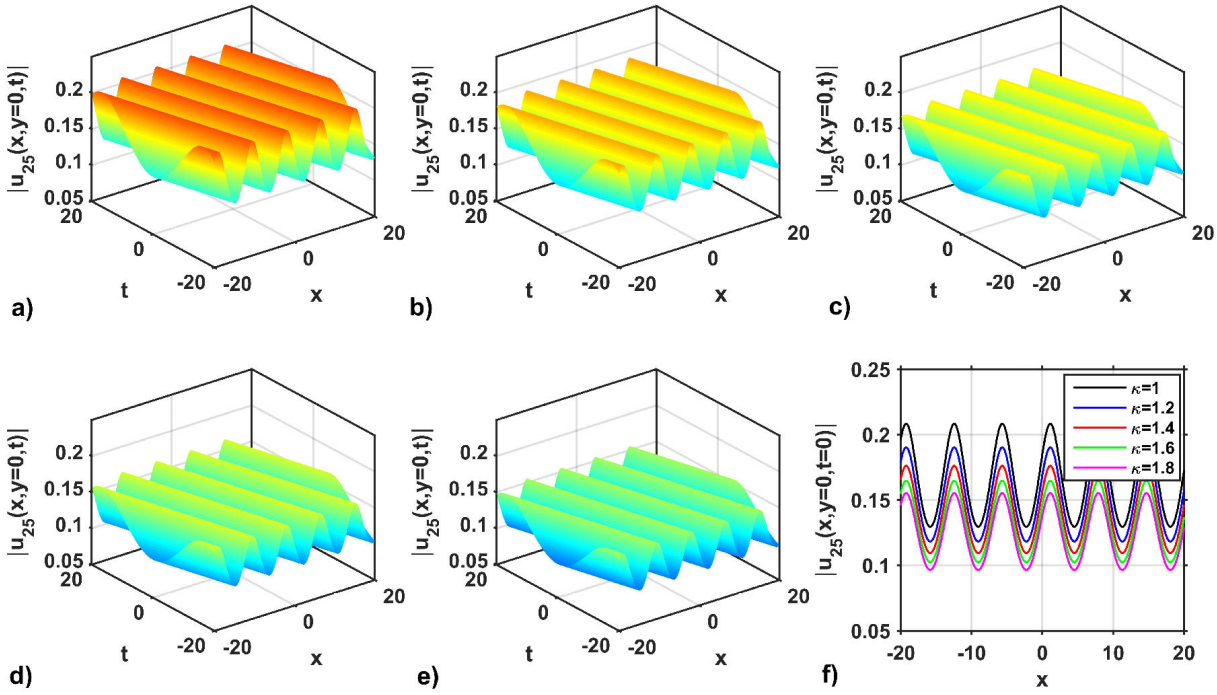

FIGURE 8. Impacts on nonlinearity of the solution $|u_{25}(x, y = 0, t)|$: a)-e) for $\kappa = 1, 1.2, 1.4, 1.6$, and 1.8, respectively, with $a = 0.15$, $b = 0.1$, $\sigma = 0.06$, $p = 1$, $q = -1$, $M = 1.1$, $P = 0.1$, $\eta = 0.1$, $m_0 = 1.5$, $\gamma = 0.03$, and f) the variation of the soliton profiles at $t = 1$ of a)-e) along with x-axis.

profile of the optical solution $u_{15}(x, y = 0, t)$. These are real and imaginary parts and modulus of the mentioned solution. Figures 3a) and b) show the 3D wave structure and represent the lump wave solution of the mentioned solution whereas Figs. 3d) and 3e) display the 2D line plots of the real and imaginary parts of the mentioned solution at $t = 0$ respectively.

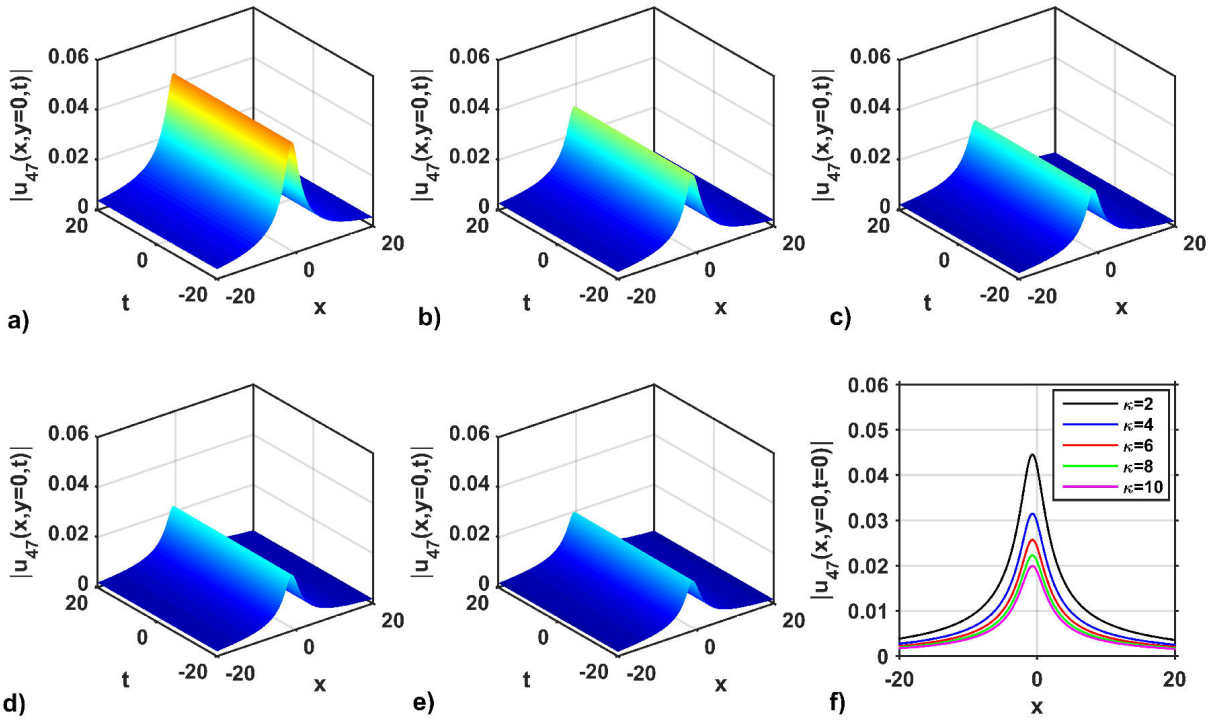

FIGURE 9. Impacts on nonlinearity of the solution $|u_{25}(x, y = 0, t)|$: a)-e) for $\kappa = 2, 4, 6, 8$, and 10, respectively, with $a = 0.15$, $b = 0.1$, $\sigma = 0.02$, $p = 1$, $q = -1$, $M = 1.1$, $P = 0.1$, $\eta = 0.1$, $m_0 = 1.5$, $\gamma = 0.03$, and f) the variation of the soliton profiles at $t = 1$ of a)-e) along with x-axis.

The modulus of the optical solution $u_{15}(x, y = 0, t)$ also demonstrate the anti-bell soliton solution, which is depicted in Fig. 2c). As shown in Fig. 2f), the 2D graph at $t = 0$ confirms this type of anti-bell soliton solution. The 3D and 2D wave structures of the solutions obtained from the KMN equation are considered to show the behavior of the solution. In addition, the 3D wave profile is exposed to show the temporal and spatial changes of the obtained optical soliton solution. The 3D wave profile for the real and imaginary parts and modulus of the optical solution $u_{41}(x, y = 0, t)$ are depicted in Figs. 4a)-c) respectively. The optical solution $u_{41}(x, y = 0, t)$ represents the periodic wave solution for the real and imaginary parts, as portrayed in Figs. 4a) and b). On the other hand, the modulus of the above solution represents the kink solution, which is depicted in Fig. 4c). The above mentioned can be confirmed from their 2D cross-sectional views at $t = 0$, as shown in Figs. 4d)-f).

4.2. Impacts of wave dispersion and nonlinearity parameters on soliton pulses

The unified method is applied to the integrable KMN equation to obtain the optical soliton solutions. The obtained solutions involve wave dispersion and nonlinearity terms. The impacts of wave dispersion and nonlinearity parameters on soliton pulses are explained graphically for showing the effectiveness of the unified method.

The impacts of wave dispersion on the attained optical solution $|u_1(x, y = 0, t)|$ is shown in Fig. 5 by selecting the free parameters as $a = 2.5$, $b = 0.2$, κ=0.01, $p = 2.5$, $q = -2.5$, $M = 0.02$, $P = 0.021$, $\eta = 1$, $m_0 = 1$, and $Y = -0.25$. For choosing the dispersion parametric values σ=0.1, 0.3, 0.5, 0.7, and 0.9, the soliton profiles of the solution $|u_1(x, y = 0, t)|$ are presented in Figs. 5a)-e), respectively. The wave profile can change for different σ values. The cross-sectional variation at $t = 1$ of the soliton profiles along the x-axis is displayed in Fig. 5f). In Fig. 5f), it can be seen that the soliton profiles along the x-axis are changed for all values of dispersion $\sigma = 0.1$, 0.3, 0.5, 0.7, and 0.9.

The amplitude of the wave profiles is increased when the value of the dispersion parameter σ decreases. Again, the 3D and 2D shapes of the wave profile of the optical solution $|u_25(x, y = 0, t)|$ is depicted in Figs. 6a)-f). As seen in Figs. 6a)-e), the 3D wave structure represents the periodic wave solution for the dispersion values $\sigma = 0.06$, 0.09, 0.12, 0.15, and 0.18, respectively, with the free parameters as $a = 1.2$, $b = 1$, $\kappa = 1$, $p = 1$, $q = 1$, $M = 0.07$, $P = 0.3$, η=1.5, $m_0 = 4.6$, and $Y = 1.5$. Figure 6f) represents the 2D combined graphs of the solution $|u_25(x, y = 0, t = 1)|$ for selecting the distinct dispersion values $\sigma = 0.06$, 0.09, 0.12, 0.15, and 0.18. In this case, it can be observed from Fig. 6f) that the amplitude of the soliton increases as the values of σ increase. It is also seen from Fig. 6f) that the signal of the wave profile solution is moved to upward positive values. However, the periods of the solitons are almost the same. Furthermore, the 3D and 2D wave profiles of the solution $|u_47(x, y = 0, t)|$ are presented in Figs. 7a)-f). The 3D wave structures of the

solution $u_47(x, y = 0, t)$ is presented in Figs. 7a)-e) for distinct dispersion values $\sigma = 0.01$, 0.05, 0.10, 0.15, and 0.2, respectively, to select the free parameter values as $a = 0.15$, $b = 0.1$, $\kappa = 1$, $p = 1$, $q = -1$, $M = 1.1$, $P = 0.1$, $\eta = 0.1$, $m_0 = 1.5$, $Y = 0.03$. The solution of $|u_{47}(x, y = 0, t)|$ represents the bell-shaped profiles. To confirm such shapes and characteristics of Figs. 7a)-e), the line variation of the profiles at $t = 1$ is shown in Fig. 7f). It is seen from the Fig. 7f) that the amplitude of the wave profiles of the solution $|u_47(x, y = 0, t = 1)|$ increases with the increase of the values σ. On the other hand, the impact of the nonlinearity parameter of solutions $|u_25(x, y, t)|$ and $|u_47(x, y, t)|$ are shown in Figs. 8 and 9, respectively. It is palpable from Figs. 8a)-e) that the intensities of the periodic wave profile decrease due to the increase of the nonlinearity parameters $\kappa = 1$, 1.2, 1.4, 1.6, and 1.8, respectively. To justify such shapes and characteristics of Figs. 8a)-e), the line variation of that profiles at $t = 1$ is presented in Fig. 8f). The same behaviors are also found and displayed for the bright shape soliton profiles, which are presented in Figs. 9a)-f). From the above mentioned discussion, it is reasonable to mention from the graphical outputs that the wave dispersion (σ) and nonlinearity (κ) parameters of the model can play a notable role in increasing and decreasing the wave profile intensity for displaying the new wave characteristics. Therefore, it is also confirmed from the above mentioned discussion that the soliton profile remains unchanged owing to the balance of the wave dispersion and nonlinearity impacts of the model. It is worth mentioning that no experimental results have been produced and compared with our produced results due to the lack of experimental equipment in our laboratory. Therefore, the choice of wave dispersion and nonlinearity parameter values of the optical solutions are predicted. For this reason, it was quite difficult to sort out the types of fiber or laser and their wavelength, which are the main limitations of our study.

5. Conclusion

Implementing the unified method to the KMN equation, we have received some new optical solutions representing the dark, bright, periodic, bell, kink, and singular solitons. We have displayed some 2D and 3D graphs of some received representative solutions including bright, dark, singular, and periodic wave solutions by selecting appropriate values of the free parameters to understand the impacts of wave dispersion and nonlinearity parameters of the KMN equation. For the bright, dark, and periodic wave solitons, it is seen that the wave amplitude increases when the wave dispersion (σ) increases. On the other hand, the wave amplitudes of the bright soliton and periodic wave decrease due to the increase in the nonlinearity parameter (κ). Thus, the amplitude of the soliton profile remains unchanged due to the balance of the wave dispersion and nonlinearity impacts of the model. The validity for the resulting outcomes was performed by substituting the attained solutions back into the equation of our choice through the use of Maple 17. Thus, the complete study approves that the executed method is a powerful tool for producing a variety of optical soliton solutions to NLEEs arising in optical fibers, and optical engineering. The outcomes obtained in this study may illuminate the researchers for further studies to understand the unseen behaviors of soliton profiles in the field of fiber optics and optical communications.

Acknowledgments

The authors would like to thank the editor of the journal and anonymous reviewer for their generous time in providing detailed comments and suggestions that helped us to improve the paper.

Compliance with ethical standards

This article does not contain any studies with human or animal subjects.

Declaration of Competing Interest

The authors declare that there is no conflict of interests concerning the publication of this manuscript.

1. J. L. Rosales, and J. L. Sánchez-Gómez, Nonlinear Schrödinger equation coming from the action of the particles gravitational field on the quantum potential, *Phys Lett A.* **166** (1992) 111, https://doi.org/10.1016/0375-9601(92)90544-V.

2. W Bao, The nonlinear Schrödinger equation and applications in Bose-Einstein condensation and plasma physics, Dynamics in Models of Coarsening, Coagulation, *Condensation and Quantization,* **9** (2007) 141.

3. C. Nadia, A. R. Seadawy and S. Chen, more general families of exact solitary wave solutions of the nonlinear Schrödinger equation with their applications in nonlinear optics, *Eur. Phys. J. Plus.* **133** (2018) 547, https://doi.org/10.1140/epjp/i2018-12354-9.

4. S. S. Chen, B. Tian, J. Chai, X. Y. Wu, and Z. Du, Lax pair, binary Darboux transformations and dark-soliton interaction of a fifth-order defocusing nonlinear Schrodinger equation for the attosecond pulses in the optical fiber communication, *Waves Random Complex Media*, **30** (2020) 389, https://doi.org/10.1080/17455030.2018.1516053.

5. H.Y. Ruan and Y.X. Chen, The study of exact solutions to the nonlinear Schrodinger equations in optical fiber, *J. Phys. Soc. Japan*, **72** (2007) 1350, https://doi.org/10.1143/jpsj.72.1350.

6. T.B. Benjamin and J.E. Feir, The disintegration of wave trains on deep water, *J Fluid Mech*. **27** (1967) 417, https://doi.org/10.1017/S002211206700045X

7. C. Coste, Nonlinear Schrödinger equation and superfluid hydrodynamics, *The European Physical Journal Condensed Matter and Complex Systems*, **1** (1998) 245, https://doi.org/10.1007/s100510050178.

8. A. Ali, A.R. Seadawy, and D. Lu, Soliton solutions of the nonlinear Schrodinger equation with the dual power law nonlinearity and resonant nonlinear Schrodinger equation and their modulation instability analysis, *Optic*, **145** (2017) 79, https://doi.org/10.1016/j.ijleo.2017.07.016.

9. H. Bulut, T.A. Sulaiman, and B. Demirdag, Dynamics of soliton solutions in the chiral nonlinear Schrodinger equation, *Nonlinear Dyn.* **91** (2018) 1985, https://doi.org/10.1007/s11071-017-3997-9.

10. D. Lu, A.R. Seadawy, J. Wang, M. Arshad, and U Farooq, Soliton solutions of the generalized third-order nonlinear Schrodinger equation by two mathematical methods and their stability. *Pranama-J. Phys.* **93** (2019) 44, https://doi.org/10.1007/s12043-019-1804-5.

11. N. Nasreen, A.R. Seadawy, D. Lu, and W.A. Albarakati, Dispersive solitary wave and soliton solutions of the generalized third order nonlinear Schrodinger dynamical equation by the modified analytical method, *Results Phys.* **15** (2019) 102641, https://doi.org/10.1016/j.rinp.2019.102641.

12. B. Gao, and Y. Wang, Complex wave solutions described by a (3+1)-dimensional coupled nonlinear Schrodinger equation with variable coefficient. *Optic*, **227** (2021) 166029, https://doi.org/10.1016/j.ijleo.2020.166029.

13. A. Kundu, and A. Mukherjee, Novel integrable higher-dimensional nonlinear Schrödinger equation: properties, solutions, applications, (2013) arXiv:1305.4023. https://doi.org/10.48550/arXiv.1305.4023.

14. A. Kundu and A. Mukherjee, T. Naskar, Modeling rogue waves through exact dynamical lamps soliton controlled by ocean currents, *Proc. R. Soc. A.* **470** (2014) 20130576, https://doi.org/10.1098/rspa.2013.0576.

15. M. Ekici, A. Sonmezoglu, A. Biswas, and M.R. Belic, Optical solitons in (2+1)-Dimensions with Kundu-Mukherjee-Naskar equation by extended trial function scheme, *Chinese J. Phys.* **57** (2019) 72, https://doi.org/10.1016/j.cjph.2018.12.011.

16. D. Qiu, Y. Zhang and J. He, The rogue wave solutions of a new (2+1)-dimensional equation. *Commun. Nonlinear Sci. Numer. Simul.* **30** (2016) 307, https://doi.org/10.1016/j.cnsns.2015.06.025.

17. N. A. Kudryashov, General solution of traveling wave reduction for the Kundu-Mukherjee-Naskar model, *Optik*. **186** (2019) 22, https://doi.org/10.1016/j.ijleo.2019.04.072.

18. A. Biswas *et al*., Optical dromions, domain walls and conservation laws with Kundu-Mukherjee-Naskar equation via traveling waves and Lie symmetry, *Results Phys.* **16** (2020) 102850, https://doi.org/10.1016/j.rinp.2019.102850.

19. Y. Yıldırım, Optical solitons to Kundu-Mukherjee-Naskar model with trial equation approach. *Optik* **183** (2019) 1061, https://doi.org/10.1016/j.ijleo.2019.02.117.

20. Y. Yıldırım, Optical solitons to Kundu-Mukherjee-Naskar model in birefringent fibers with trial equation approach. *Optik* **183** (2019) 1026, https://doi.org/10.1016/j.ijleo.2019.02.141.

21. A. Jhangeer, A.R. Seadawy, F. Ali, A. Ahmed, New complex waves of perturbed Shrödinger equation with Kerr law nonlinearity and Kundu-Mukherjee-Naskar equation, *Results Phys.* **16** (2020) 102816, https://doi.org/10.1016/j.rinp.2019.102816.

22. A.I. Aliyu, Y. Li, D. Baleanu, Single and combined optical solitons, and conservation laws in (2+1)-dimensions with Kundu-Mukherjee-Naskar equation. *Chinese Journal of Physics.* **63** (2020) 410, https://doi.org/10.1016/j.cjph.2019.11.001.

23. Y. Yıldırım, M. Mirzazadeh, Optical pulses with Kundu-Mukherjee-Naskar model in fiber communication systems. *Chinese Journal of Physics*. **64** (2020) 183, https://doi.org/10.1016/j.cjph.2019.10.025.

24. H. Gunerhan, F.S. Khodadad, H. Rezazadeh, and M.M.A. Khater, Exact optical solutions of the (2+1)-dimensions Kundu-Mukherjee-Naskar model via the new extended direct algebraic method, *Mod. Phys. Lett. B.* **34** (2020) 2050225, https://doi.org/10.1142/S0217984920502255.

25. R.A. Talarposhti *et al*., Optical soliton solutions to the (2+1)-dimensional Kundu-Mukherjee-Naskar equation, *Int. J. Mod. Phys. B.* **34** (2020) 2050102, https://doi.org/10.1142/S0217979220501027.

26. D. Kumar *et al*., Optical solutions to the Kundu-Mukherjee-Naskar equation: mathematical and graphical analysis with oblique wave propagation, *Phys. Scr.* **96** (2021) 025218, https://doi.org/10.1088/1402-4896/abd201.

27. S. Akcagil, and T. Aydemir, A new application of the unified method, new trends. *Math. Sci.* **6** (2018) 185, http://dx.doi.org/10.20852/ntmsci.2018.261.

28. O. M. Gözükızıl, S. Akçağıl, and T. Aydemir, Unification of all hyperbolic tangent function methods, *Open Phys.* **14** (2016) 524, https://doi.org/10.1515/phys-2016-0051.

29. L. Huibin, and W. Kelin, Exact solutions for some coupled nonlinear equations II, *J. Phys. A: Math General* **23** (1990) 4197, https://doi.org/10.1088/0305-4470/23/18/015.

30. W. Malfliet, and W. Hereman, The tanh method. I: Exact solutions of nonlinear evolution and wave equations, *Phys. Scr.* **54** (1996) 563, https://doi.org/10.1088/0031-8949/54/6/003.

31. W. Malfliet, and W. Hereman, The tanh method. II: Perturbation technique for conservative systems, *Phys. Scr.* **54** (1996) 569, https://doi.org/10.1088/0031-8949/54/6/004.

32. E. G. Fan, Extended tanh-function method and its applications to nonlinear equations, *Phys Lett. A.* **277** (2000) 212, https://doi.org/10.1016/S0375-9601(00)00725-8.

33. S. A. El-Wakil, S. K. El-Labany, M. A. Zahran, and R. Sabry, Modified extended tanh-function method and its applications to nonlinear equations, *Appl. Math. Comput.* **161** (2005) 403, https://doi.org/10.1016/j.amc.2003.12.035.

34. S. A. Khuri, A complex tanh-function method applied to nonlinear equations of Schrödinger type, Chaos, *Solitons Fractals.* **20** (2004) 1037, https://doi.org/10.1016/j.chaos.2003.09.042.

35. M. Nuruzzaman, D. Kumar, and G. C. Paul, Fractional low-pass electrical transmission line model: Dynamic behaviors of exact solutions with the impact of fractionality and free parameters. *Results in Physics.* **27** (2021) 104457, https://doi.org/10.1016/j.rinp.2021.104457.

36. D. Kumar, C. K. Kuo, G. C. Paul, J. Saha, and I. Jahan, Wave propagation of resonance multi-stripes, complexitons, and lump and its variety interaction solutions to the (2+1)-dimensional pKP equation. *Communications in Nonlinear Science and Numerical Simulation.* **100** (2021) 105853, https://doi.org/10.1016/j.cnsns.2021.105853.

37. D. Kumar, I. Raju, G. C. Paul, M. E. Ali, and M. D. Haque, Characteristics of lump-kink and their fission-fusion interactions, and rogue and breather wave solutions for a (3+1)-dimensional generalized shallow water equation. *International Journal of Computer Mathematics.* **99** (2022) 714. https://doi.org/10.1080/00207160.2021.1929940.

38. D. Kumar, K. Hosseini, M. K. Kaabar, M. Kaplan, and O. Salahshour, On some novel solution solutions to the generalized Schrödinger-Boussinesq equations for the interaction between complex short wave and real long wave envelope. *Journal of Ocean Engineering and Science.* **7** (2022) 353. https://doi.org/10.1016/j.joes.2021.09.008.

39. D. Kumar, A. K. Joardar, A. Hoque, and G. C. Paul, Investigation of dynamics of nematicons in liquid crystals by extended sinh-Gordon equation expansion method. *Opt Quantum Electron.* **51** (2019) 212, https://doi.org/10.1007/s11082-019-1917-6.

40. S. M. R. Islam, K. Khan, and K. M. A. Woadud, Analytical studies on the Benney-Luke equation in mathematical physics. *Waves Random Complex Media.* **28** (2018) 300, https://doi.org/10.1080/17455030.2017.1342880.

41. S. M. R. Islam, M. H. Bashar, and M. Noor, Immeasurable soliton solutions and enhanced $\frac{G'}{G}$-expansion method. *Phys Open.* **9** (2021) 100086, https://doi.org/10.1016/j.physo.2021.100086.

42. S. M. R. Islam, Application of an enhanced $\frac{G'}{G}$-expansion method to find exact solutions of nonlinear PDEs in particle physics. *Am. J. Appl. Sci.* **12** (2015) 836, https://doi.org/10.3844/ajassp.2015.836.846.

43. M. H Bashar, S. M. R. Islam, and D. Kumar, Construction of traveling wave solutions of the (2+1)-Dimensional Heisenberg ferromagnetic spin chain equation. *Partial Diff. Eqs. Appl. Math.* **4** (2021) 100040, https://doi.org/10.1016/j.padiff.2021.100040.

44. M.H. Bashar, and S.M.R. Islam, Exact solutions to the (2+1)-Dimensional Heisenberg ferromagnetic spin chain equation by using modified simple equation and improve F-expansion methods. *Phys Open.* **5** (2020) 100027, https://doi.org/10.1016/j.physo.2020.100027.

45. S. U. Rehman, M. Bilal and J. Ahmad, New exact solitary wave solutions for the 3D-FWBBM model in arising shallow water waves by two analytical methods. *Results Phys* **25** (2021) 104230, https://doi.org/10.1016/j.rinp.2021.104230.

46. R. F. Zhanh, M. C. Li, M. Albishari, F. C. Zheng and Z. Z. Lan, Generalized lump solutions, classical lump solutions and rough waves of the (2+1)-dimensional Caudrey-Dodd-Gibbon-Kotera-Sawada-like equation. *Appl. Math. Comput.* **403** (2021) 126201, https://doi.org/10.1016/j.amc.2021.126201.

47. K. U. Tariq *et al.*, On new closed form solutions: The (2+1)-dimensional Bogoyavlenskii system Mod. *Phys. Lett. B.* **35** (2021) 2150150, https://doi.org/10.1142/S0217984921501505.